







# Leveraging Dynamic Stackelberg Pricing Game for Multi-Mode Spectrum Sharing in 5G-VANET

Bo Qian , *Student Member, IEEE*, Haibo Zhou , *Senior Member, IEEE*, Ting Ma , Yunting Xu , Kai Yu , Xuemin Shen , *Fellow, IEEE*, and Fen Hou, *Member, IEEE*

**Abstract**—5G enabled Vehicular ad hoc network (5G-VANET) plays a promising role to support diverse intelligent transportation system (ITS) applications. There are three types of communication modes in 5G-VANET: cellular mode, reuse mode and dedicated mode, i.e., vehicle users (VUEs) communicate with each other using the cellular network spectrum directly, in an underlay sharing way, and utilizing the allocated dedicated spectrum, respectively. However, how to dynamically share the multi-mode spectrum to optimize the network performance (i.e., network throughput) in 5G-VANET is a challenging task due to the high dynamic VANET environment and network resource heterogeneity. In this paper, we propose a dynamic Stackelberg pricing game enabled multi-mode spectrum sharing solution in 5G-VANET. In specific, we develop an access price strategy for different spectrum sharing modes considering the cellular BS's revenue and whole network throughput, while VUEs can select communication modes in a distributed way and dynamically change the selections through an evolutionary game. Through testing different traffic scenarios generated by SUMO, we demonstrate the effectiveness of the proposed algorithm. Specifically, the proposed algorithm can improve the total transmission rate of VANET by at least 20% compared with the random selection method.

**Index Terms**—5G, VANET, spectrum sharing, mode selection, Stackelberg pricing game, evolutionary game.

## I. INTRODUCTION

**5G** enabled Vehicular ad hoc network (5G-VANET) is expected to support a variety of vehicular services related to location, communications, computing and security [1]–[3]. The FCC's 5G Fast Plan [4], which outlines strategies

Manuscript received November 22, 2019; revised February 19, 2020; accepted March 10, 2020. Date of publication April 13, 2020; date of current version June 18, 2020. This work was supported in part by the National Natural Science Foundation of China under Grant 61871211, in part by Natural Science Foundation Jiangsu Province Youth Project under Grant BK20180329, in part by Innovation and Entrepreneurship of Jiangsu Province High-level Talent Program, in part by Summit of the Six Top Talents Program Jiangsu Province, in part by Natural Sciences and Engineering Research Council of Canada (NSERC), and in part by Macau Science and Technology Development Fund and the Ministry of Science Technology of the Peoples Republic of China under Grant 037/2017/AMJ. The review of this article was coordinated by Prof. G. Gui. (*Corresponding author: Haibo Zhou.*)

Bo Qian, Haibo Zhou, Ting Ma, Yunting Xu, and Kai Yu are with the School of Electronic Science and Engineering, Nanjing University, Nanjing 210023, China (e-mail: boqian@smail.nju.edu.cn; haibozhou@nju.edu.cn; majiawan27@163.com; yuntingxu@smail.nju.edu.cn; kaiyu@smail.nju.edu.cn).

Xuemin Shen is with the Department of Electrical and Computer Engineering, University of Waterloo, Waterloo, Ontario N2L 3G1, Canada (e-mail: sshen@uwaterloo.ca).

Fen Hou is with the State Key Laboratory of IoT for Smart City and Department of Electrical and Computer Engineering, University of Macau, Taipa 999078, China (e-mail: fenhhou@um.edu.mo).

Digital Object Identifier 10.1109/TVT.2020.2987014

for modifying spectrum policies, infrastructure policies, and existing regulations, makes additional spectrum available for 5G services, including the VANET. In order to fully utilize the newly released spectrum and to meet the growing and tremendous demands of vehicular communications, it is crucial to enable high-rate and reliable vehicular wireless access in a scalable and cost-effective manner in light of emerging 5G technologies [5]–[7].

With the rapid development of VANET and the sharp growth of abundant vehicular services [8], [9], the vehicular spectrum scarcity problem will become more and more urgent in the foreseeable future. In third-generation partnership project (3GPP) Release 15 [10], the vehicle-to-everything (V2X) functionalities are expanded to support 5G. The cellular V2X (C-V2X) includes support of both direct communication of vehicle-to-vehicle (V2V) and traditional cellular-network based communication. The direct communication between vehicle and other devices uses so-called PC5 interface. In addition to the direct communication over PC5, C-V2X also allows the C-V2X device to use the cellular network connection in the traditional manner over Uu interface. Uu refers to the logical interface between the UE and the base station (BS), which is generally referred to as vehicle-to-network (V2N). In 5G-VANET, they can utilize the licensed cellular frequency band to transmit the messages either through the cellular BS or directly with each other. Additionally, they can use the dedicated spectrum allocated for 5G vehicular communication by countries [11]. For example, China has divided 20 MHz of spectrum in 5905-5925 MHz as a dedicated spectrum for LTE-V communications. In summary, the vehicular communication modes in 5G-VANET can be divided into the following three types and a list of comparison is shown in Table I [12]–[14]:

- *Cellular mode*: VUEs transmit the messages with the aid of cellular BS using Uu interface. VUEs with cellular mode are similar to traditional cellular users [15].
- *Reuse mode*: VUEs directly transmit data to each other reusing the subchannels of cellular users in an underlay spectrum sharing way [16], [17].
- *Dedicated mode*: VUEs directly communicate with each other using PC5 interface in the dedicated frequency band [5], e.g., 5905-5925 MHz in China.

Currently, there is no systematic study for the mode selection of VUEs and the performance analysis in 5G-VANET. However, analyzing this three-mode selection problem is very significant for the performance of VANET in the next-generation 5G networks. Regarding the challenge of this topic, we conduct the following analysis. First, we must be aware of different unique

mobility patterns between VUEs and traditional cellular users, which would greatly impact the network performance. Second, considering the different mobility behaviors, vehicles must follow fixed road motions, in which their distribution cannot be modeled by the traditional Poisson point process (PPP) [18]. The VUEs' interference and channel condition need to be remodeled when analyzing the performance of each mode. Last but not least, the real-time requirement is supposed to be very high for the mode selection of VUEs. It is necessary to explore a new and applicable efficient algorithm for mode selection in 5G-VANET.

It has been proved that providing economic incentives to users involved is essential for the success of dynamic spectrum access [19]. In order to jointly deal with the three-mode selection problems of VUEs and the spectrum sharing of the cellular BS in 5G-VANET, we propose a dynamic Stackelberg pricing game framework, where the cellular BS acts as the leader and potential VUEs<sup>1</sup> serve as followers. The transmission power of each VUE is regulated by a channel inversion power control model [20], [21], where the received power is required to be a fixed threshold. Especially, the adaptive three-mode selection strategy of potential VUEs is formulated as an evolutionary game, in which the objective of each VUE is to maximize its own payoff. The adaptation process of VUEs' distribution is formulated as replicator dynamics, based on which we propose a VUEs-controlled mode selection algorithm with a solution of evolutionary stable strategy (ESS). Considering the effect of replicator dynamics on VUEs' distribution, we formulate the optimal dynamic pricing problem of the cellular BS as a leader control, which aims to optimize the benefit from the economic revenue and the 5G-VANET performance deviation.

Now we highlight the novelty and contributions in three-fold as follows.

- *The dynamic Stackelberg pricing game framework:* In order to jointly solve the three-mode selection and access pricing problem of the cellular BS, we combine the benefits of the BS with the VUE's payoff to maximize the performance of the 5G-VANET by dynamically adjusting the access price of each mode. Under this framework, VUEs can quickly reach a convergent solution, which meets the high-dynamic access environment of the VANET.
- *A novel theoretical analysis combining stochastic geometry and game theory in 5G-VANET:* By integrating the stochastic geometry tools and the game theory, we propose a novel method to analyze the performance of the three-mode selection in 5G-VANET. Especially, we take advantage of the stochastic geometry-based theoretical approach to model and analyze the performance and relationship between VUEs' mode selection and access pricing of the cellular BS.
- *The optimal distribution and ESS for the 5G-VANET:* Through theoretical analysis and numerical experiments, it is proved that our algorithm could achieve the expected

results. Particularly, although the three-mode selection strategies are carried out in a user-controlled manner, the dynamic pricing of the cellular BS could be regarded as an incentive mechanism to induce VUEs' distribution to a pre-determined value, which is also an ESS. In particular, simulations show that it can improve the total transmission rate of VANET by at least 20% compared with the random selection method.

The remainder organizations of this paper are as follows. We first review related works in Section II. Then, we describe our system model, including network model, system assumptions and the dynamic Stackelberg pricing game framework in Section III. The average rate analysis of the three modes is presented in detail in Section IV. In Section V, we propose an evolutionary game for the follower's three-mode selection. The leader control problem, i.e., dynamic pricing of the cellular BS, is formulated in Section VI. We conduct extensive numerical experiments in Section VII. Finally, we make a conclusion and propose some future work in Section VIII.

## II. RELATED WORKS

In the last few years, with the rapid development of the intelligent transportation system (ITS), vehicular communication network (as one of the next generation networks) has been widely studied. In particular, as the 5G-VANET is assigned a specific spectrum in the LTE cellular network, multi-mode selection issues are increasingly being investigated. Although there has been some research in the field of separate cellular networks and dedicated short-range communications (DSRC), their cross-domain research is still in its infancy [22]. In general, these existing multi-mode selection algorithms could be divided into two categories, i.e., centralized schemes [23], [24] and distributed schemes [25], [26].

In the centralized schemes, the cellular BS needs to acquire the link status of all users and then decides an appropriate communication mode for each user. In [23], Zhu *et al.* proposed a dynamic Stackelberg game framework to jointly address the problems of spectrum partitioning and mode selection. Although the three-mode selection algorithm is proposed, the most important performance modeling could not be applied to the 5G-VANET. Also, the access prices of each mode are fixed in their paper. In [24], with the aim of enhancing the offloading capacity of cellular-assisted device-to-device (D2D) communication, Ma *et al.* considered three D2D communication modes, including direct mode, relay-assisted mode, and local route mode. Although they formulated a unified model for the three-mode selection problem, the proposed scheduling algorithm is too straightforward and dependent on the BS. Basically, the BS was considered to estimate the achievable data rate and select the optimal mode with a maximal data rate for each D2D pair in three modes.

In comparison with the centralized BS-controlled schemes, the distributed user-controlled algorithms usually have lower computational complexity and signaling overhead. In [25], Wu *et al.* studied a Stackelberg pricing game framework to solve the joint pricing and power allocation in dynamic spectrum

<sup>1</sup>According to the communication distance limitation, some VUEs with far distances can only choose the cellular mode, here, we denote VUEs as the potential VUEs that can make mode selection among the above three types of vehicular communication.

TABLE I  
COMPARISON OF COMMUNICATION MODES IN 5G-VANET

Features	Cellular mode	Reuse mode	Dedicated mode
Transmit mode	V2I	V2V	V2V
Interface	Uu	PC5	PC5
Spectrum band	Licensed band	Licensed band	Dedicated band <sup>1</sup>
Speed support	$\leq 350$ km/h	$\leq 140$ km/h	$\leq 140$ km/h
Data rate	$\leq 300$ Mb/s	3-27 Mb/s	3-27 Mb/s

<sup>1</sup>The dedicated band for V2X communication is 5905-5925 MHz in China.

access networks, and proposed a distributed algorithm with an incentive-compatible mechanism to find the equilibrium with social welfare optimum cooperatively. In [27], Niyato *et al.* used evolutionary games into the distributed mode selection problem and compared with reinforcement-learning algorithms, which showed that the dynamics of network selection could be captured by the replicator dynamics of the evolutionary game. Omri and Hasna [26] proposed a distance-based mode selection scheme for D2D-enabled cellular networks, which was based on an average threshold between two users to trigger the D2D mode. In this paper, they considered a tractable analytical model for mode selection in moving D2D scenarios.

Recently, there are also some research focusing on the advance of spectrum sharing problem in 5G-VANET [5], [14], [21], i.e., the dynamic sharing of licensed and unlicensed wireless spectrum, including the underlay shared cellular spectrum, TV white space (TVWS), and DSRC. In [21], Chen *et al.* studied the performance of vehicular device-to-device (V-D2D) mode and cellular mode considering an urban area in a grid-like street and employed a joint power control and mode selection scheme. They were the first to use a stochastic geometry method to innovatively analyze the performance of V-D2D mode and cellular mode between VUEs for the 5G-VANET, while the assumption that all V-D2D and cellular VUEs use the total spectrum bandwidth of the BS (does not divide orthogonal subchannels) might weaken their practical value. In [5], Zhou *et al.* proposed an adaptive vehicular data piping framework for the joint utilization of TV white space (TVWS) spectrum and DSRC. They considered three types of vehicular data pipes, i.e., TVWS, DSRC and cellular, where the cellular data pipe was considered to be a control link to coordinate the dynamic selection of TVWS and DSRC spectrum. In essence, there is still no solution to the choice of the three modes in their work. It is crucial to design the 5G spectrum sharing architecture and propose optimal dynamic vehicular access solutions when multiple wireless vehicular access techniques coexist.

### III. SYSTEM MODEL

As shown in Fig. 1, we consider a 5G-VANET system in the highway scenario, where VUEs can communicate with each other using one of three modes: cellular mode, reuse mode, and dedicated mode. In order to study the impact of mode selection on network performance, we need to analyze the average transmission rate of VUEs in each mode based on a specific motion model. The theoretical analysis of VANET is a challenging research problem due to the unique mobility patterns. The vehicular communication in the highway scenario is considered

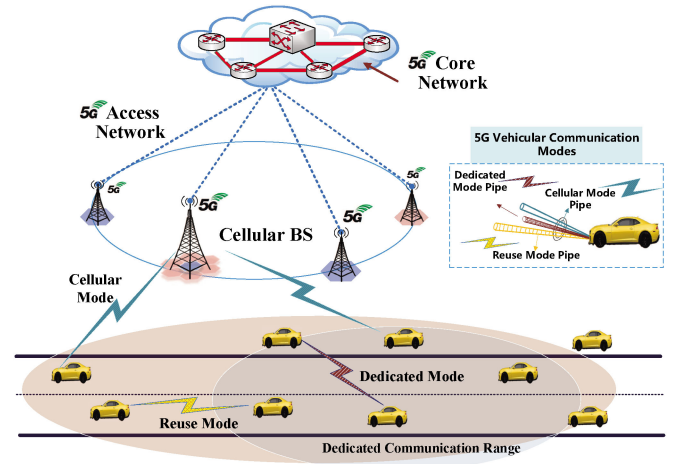


Fig. 1. Multi-mode vehicular communications scenario in 5G-VANET.

TABLE II  
A LIST OF MAJOR SYMBOLS

Notation	Description
$\lambda, v$	The density and speed of VUE flow, respectively.
$L$	Length of highway segment, also coverage range of BS.
$L_0, L_{\max}$	Shortest and largest distances from BS to highway road.
$D$	Threshold distance for a VUE becoming a potential VUE.
$P_r^{\max}$	Maximum transmission power of VUE in reuse mode.
$T$	The time horizon for the mode selection.
$N_r, N$	Number of total requesting VUEs and potential VUEs.
$F, B$	Subchannel Number and bandwidth for each subchannel.
$\eta_c, \eta_r$	Path-loss exponent of cellular and reuse mode.
$\rho_c, \rho_r$	The receive power threshold of cellular and reuse mode.
$h, W_0$	Fading gain and noise power.
$\mathcal{M}$	Mode selection strategy set of potential VUEs.
$\Phi_r^l$	Set of interfering VUEs of reuse mode in subchannel $l$ .
$I_c^l, I_r^l$	Interference of subchannel $l$ for cellular and reuse mode.
$\mathcal{L}_{Pl}(\cdot)$	Laplace transform of PDF of interferences $I^l$ .
$\mathbf{E}(\cdot)$	The expectation of a random variable.
$\tau_i$	Average rate of a VUE choosing mode $i$ .
$\mathbf{p}$	Dynamic pricing of three modes.
$\mathbf{x}$	Population profile of potential VUEs.
$\pi(i, \mathbf{x}, \mathbf{p})$	Payoff of a potential VUE choosing mode $i$ .
$\mathcal{U}(\mathbf{x}, \mathbf{p})$	The instantaneous payoff of the BS.

as an example to systematically investigate, and other scenarios can be studied with similar technologies. In this section, we first describe the VUE mobility pattern and the network model. Then, the mode selection probability and resource allocation schemes are presented. A summary of notations is given in Table II.

#### A. Vehicular Mobility Model and Channel Model

We take the highway scenario (shown in Fig. 1) as an example to model, since it is the most typical and common scenario for the 5G-VANET. According to [5], the relation between the VUE density  $\lambda$  and speed  $v$  is given by  $v = v_{\max}(1 - \lambda/\lambda_{\max})$ , where  $\lambda_{\max}$  and  $v_{\max}$  denote the maximum values of vehicle density and speed, respectively. In addition, on basis of [28], the steady-state distribution of vehicles location approaches a uniform distribution, i.e.,  $V_i \sim U[0, L]$ , where  $L$  is the length of the highway segment. Consequently, the V2V distances at each time step are i.i.d. with a triangular distribution, whose



Probability Density Function (PDF)  $f_{V2V}(x)$  is:

$$f_{V2V}(x) = \frac{2}{L} \left(1 - \frac{x}{L}\right), \quad 0 < x \leq L. \quad (1)$$

Then, by integrating (1), the Cumulative Distribution Function (CDF) of V2V distance is given as  $F_{V2V}(x) = \frac{2}{L}(x - \frac{x^2}{2L})$ .

In this paper, a general power-law path-loss model [20], [29] is considered with the decay rate  $d^{-\eta}$ , where  $d$  indicates the distance between transmitter and receiver and  $\eta$  represents the path-loss exponent. Particularly, we denote  $\eta_c$  and  $\eta_r$  as the path-loss exponent for cellular mode and reuse mode, respectively. In our framework, the transmission power of VUEs is regulated by a simple yet effective mechanism, named channel inversion power control model [20], [21], where the received signal power is required to equal a certain receive power threshold  $\rho_i$ ,  $i = c, r$  for cellular mode and reuse mode, respectively. Hence, we express the received power as  $\rho_i h$ , where  $h$  is the channel gain. We consider Rayleigh fading model [18] and the channel gain satisfies  $h \sim \exp(1)$ . Given the maximum transmission power and receive power in reuse mode (i.e.,  $P_r^{\max}$  and  $\rho_r$ ), we derive the maximum transmission distance in reuse mode  $D = (\frac{P_r^{\max}}{\rho_r})^{\frac{1}{\eta_r}}$ , where  $\eta_r$  represents the path-loss exponent of the reuse mode. According to the distribution of V2V distance, the PDF of transmission distance in reuse mode is a truncation of (1):

$$f_{Reuse}(x) = \beta \frac{2}{L} \left(1 - \frac{x}{L}\right), \quad 0 < x \leq D, \quad (2)$$

where  $\beta \triangleq \frac{1}{F_{V2V}(D)} = \frac{L^2}{2DL - D^2}$ . And the probability that the distance of V2V is less than D is:

$$\mathbb{P}(d \leq D) = \int_0^D f_{V2V}(x) dx = F_{V2V}(D) = \frac{2}{L} \left(D - \frac{D^2}{2L}\right).$$

From the uniform distribution of VUEs' location, i.e.,  $V_i \sim U[0, L]$ , the distance from the VUE to the midpoint of the road segment is also a uniform distribution, i.e.,  $l \sim U(-\frac{L}{2}, \frac{L}{2})$ . Denote the shortest and largest distances from the BS to the highway road are  $L_0$  and  $L_{\max} = \sqrt{\frac{L^2}{4} + L_0^2}$ , respectively. The PDF of vehicle-to-BS (V2B) distance is:

$$f_{V2B}(x) = \frac{2x}{L\sqrt{x^2 - L_0^2}}, \quad L_0 \leq x \leq L_{\max}.$$

### B. Transmission Power of VUEs in Cellular and Reuse Modes

According to the distance distributions and channel inversion power control model, we can derive the PDF of VUEs' transmission power in cellular and reuse modes. Denote  $d_c$  and  $d_r$  as the transmission distances of VUEs in cellular and reuse modes, respectively. For cellular mode, given the received power  $\rho_c h$ , we can deduce the transmission power as  $P_c^{tr} = \rho_c d_c^{\eta_c}$ . Then, the CDF of transmission power of VUEs in cellular mode is:

$$\begin{aligned} \mathbb{P}(P_c^{tr} \leq p) &= \mathbb{P}(\rho_c d_c^{\eta_c} \leq p) = \mathbb{P}\left(d_c \leq \left(\frac{p}{\rho_c}\right)^{\frac{1}{\eta_c}}\right) \\ &= \int_{L_0}^{\left(\frac{p}{\rho_c}\right)^{\frac{1}{\eta_c}}} \frac{2x}{L\sqrt{x^2 - L_0^2}} dx = \frac{2}{L} \sqrt{\left(\frac{p}{\rho_c}\right)^{\frac{2}{\eta_c}} - L_0^2}. \end{aligned} \quad (3)$$

Then, the PDF of transmission power for cellular mode is:

$$f_{Cellular, tr}(x) = \frac{2\rho_c^{-\frac{2}{\eta_c}} x^{\frac{2}{\eta_c}-1}}{L\eta_c \sqrt{\left(\frac{x}{\rho_c}\right)^{\frac{2}{\eta_c}} - L_0^2}}, \quad \rho_c L_0^{\eta_c} \leq x \leq \rho_c L_{\max}^{\eta_c}.$$

Similarly, for reuse mode, given the received power  $\rho_r h$ , we could deduce the transmission power as  $P_r^{tr} = \rho_r d_r^{\eta_r}$ . Then, the CDF of transmission power in reuse mode is:

$$\begin{aligned} \mathbb{P}(P_r^{tr} \leq p) &= \mathbb{P}(\rho_r d_r^{\eta_r} \leq p) = \mathbb{P}(d_r \leq \left(\frac{p}{\rho_r}\right)^{\frac{1}{\eta_r}}) \\ &= \int_0^{\left(\frac{p}{\rho_r}\right)^{\frac{1}{\eta_r}}} \beta \frac{2}{L} \left(1 - \frac{x}{L}\right) dx = \beta \frac{2}{L} \left[ \left(\frac{p}{\rho_r}\right)^{\frac{1}{\eta_r}} - \frac{\left(\frac{p}{\rho_r}\right)^{\frac{2}{\eta_r}}}{2L} \right]. \end{aligned}$$

Hence, the PDF of transmission power in reuse mode is:

$$\begin{aligned} f_{Reuse, tr}(x) &= \frac{2\beta}{L^2 \eta_r \rho_r} \left[ L \left(\frac{x}{\rho_r}\right)^{\frac{1}{\eta_r}-1} - \left(\frac{x}{\rho_r}\right)^{\frac{2}{\eta_r}-1} \right], \\ 0 \leq x \leq P_r^{\max}. \end{aligned} \quad (4)$$

### C. Spectrum Allocation Schemes

We assume that the available frequency spectrum of the cellular BS consists of  $F$  subchannels, each of which has a spectral bandwidth  $B$  Hz. Meanwhile, three communication modes have different spectrum allocation schemes, which are usually introduced in cellular networks [20], [23], [30]. For the cellular mode, we assume that the BS schedules the spectrum resource in a round-robin (RR) manner, which results in an equal sharing of spectrum resources for VUEs in this mode. For the reuse mode, each potential VUE randomly chooses  $k$  out of  $F$  subchannels as candidates. For each chosen candidate subchannel, the VUE decides to transmit in it with an independent probability  $p_m$ , which is denoted as the medium access probability (MAP) [30]. This scheme means that the VUE can multiplex multiple subchannels simultaneously for transmission in the reuse mode. According to this allocation scheme, the probability of selecting the subchannel  $l \in \{F\}$  as a candidate is  $p_l = \frac{C_F^k - C_{F-1}^k}{C_F^k} = \frac{k}{F}$  and the access probability is  $p_l p_m$ . For the dedicated mode, since its frequency spectrum is specific and refers to the existing DSRC (i.e., IEEE 802.11p), all potential VUEs in this mode compete for information transmission through the carrier sense multiple access with collision avoidance (CSMA/CA) scheme [31].

### D. Dynamic Stackelberg Pricing Game

Since the decision of the cellular BS about access prices and mode selections of VUEs depend on each other, a dynamic Stackelberg pricing game is proposed to model their interaction. The proposed dynamic (i.e., time-dependent) Stackelberg pricing game consists of a BS (leader) dynamic pricing optimization and a group of potential VUEs (followers) using evolutionary game. As shown in Fig. 2, the decision period  $T$  is divided into multiple decision points. At each round, the BS first decides access prices, and then VUEs select modes.

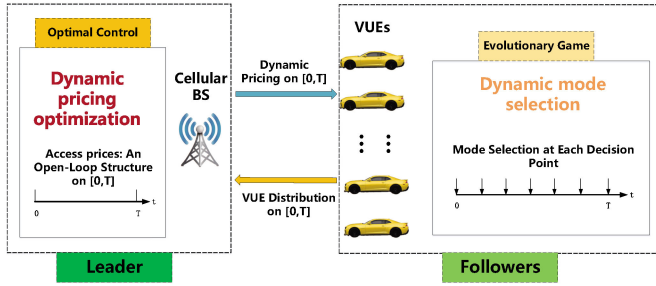


Fig. 2. Dynamic Stackelberg pricing game framework in multi-mode spectrum sharing in 5G-VANET.

1) *Dynamic Pricing Control of the Leader*: Taking into account the three-mode selection strategies of potential VUEs, the cellular BS is supposed to dynamically control the access prices to satisfy the BS's profit and induce VUEs' distribution to an optimal proportion (e.g., maximum sum-rate) of the 5G-VANET. In this way, we denote access prices  $p(t)$  as a function of time in  $[0, T]$  and model the dynamic pricing as a leader control for the cellular BS. In order to obtain the optimal pricing  $p(t)$ , the leader must consider the followers' response to the leader control, through predicting the behavior of VUEs during the evolution game. As shown in Fig. 2, the cellular BS calculates the dynamic pricing  $p(t)$ ,  $t \in [0, T]$  in advance with an open-loop structure, and VUEs need to return their mode selection strategies at each decision point.

2) *Three-Mode Selection of the Followers*: Once received the dynamic pricing  $p(t)$  broadcasted by the BS, potential VUEs would independently select communication modes. Meanwhile, they can dynamically change their modes to maximize their own payoffs through jointly considering the average transmission rate and the access prices. The average transmission rate of a communication mode also relies on the potential VUEs' proportion, which means the selections of VUEs interact with each other. Considering the lack of global messages and strong computing power for a vehicular device, we assume that VUEs have bounded rationality, in which decision-makers are seeking a satisfactory solution rather than an optimal one. We are prompted by these characteristics to model the selection of potential VUEs using an evolutionary game, which is specifically designed to analyse the behavior of players with bounded rationality.

3) *Time Scale of Scheduling*: We divide the time period  $[0, T]$  into some decision points, at which each potential VUE chooses its adaptive strategy. The proposed dynamic Stackelberg pricing game is supposed to be carried out every  $T$  time interval. Note that there is a trade-off between the size of  $T$  and the state of the network. The smaller the  $T$ , the more the algorithm can adapt to the dynamic transformation of the 5G-VANET, but the computation load will be heavier.

#### IV. PERFORMANCE ANALYSIS OF MULTI-MODE 5G-VANET SPECTRUM SHARING

In this section, we analyze the average achievable rate of VUEs in each communication mode, i.e., cellular mode, reuse mode and dedicated mode, using stochastic geometry tools.

#### A. Average Transmission Rate of VUEs in Cellular Mode

In order to calculate the average transmission rate in cellular mode, we first calculate the interference to derive the SINR, and then draw the conclusion using the Shannon's formula.

Denote  $N_r$  as the set of requesting VUEs under consideration,  $x = [x_c, x_r, x_d]$  as the distribution of cellular, reuse and dedicated mode, respectively. Since both the reuse mode and the dedicated mode belong to the V2V communication, their maximum communication distance is the same. Then, the number of V2V pairs in the three mode is  $N_{Cellular} = N_r(1 - \mathbb{P}(d \leq D)) + N_r \mathbb{P}(d \leq D)x_c$ ,  $N_{Reuse} = N_r \mathbb{P}(d \leq D)x_d$  and  $N_{Dedicated} = N_r \mathbb{P}(d \leq D)x_d$  respectively. The number of potential VUEs is  $N = N_r \mathbb{P}(d \leq D)$ .

When a potential VUE of cellular mode accesses channel  $l$ , the interference comes from other VUEs in reuse mode using channel  $l$  in  $\Phi_r^l$ . Then, the aggregate interference suffered by the receiver is given by  $I_c^l = \sum_{X_i \in \Phi_r^l} P_r h_r d_c^{-\eta_r}$ , where  $h_r$  denotes the fading gain from  $X_i$  to the receiver, and  $d_c$  represents the distance from  $X_i$  to the cellular BS. In this case, the SINR of the receiver could be represented as follows:

$$\text{SINR}_c^l = \frac{P_c h_c d_c^{-\eta_c}}{I_c^l + W_0} = \frac{\rho_c h_c}{I_c^l + W_0}, \quad (5)$$

where  $h_c$  represents the fading gain from its transmitter to the receiver,  $W_0$  is the noise power.

Using stochastic geometry tools, we have following results. Given VUEs distribution  $\mathbf{x} = [x_c, x_r, x_d]$ , the coverage probability  $p_c(\mathbf{x}, v)$  of a VUE with the cellular mode is as follows:

$$\begin{aligned} p_c(\mathbf{x}, v) &= \mathbb{P}(\text{SINR}_c^l > v) = \mathbb{P}\left(h_c > \frac{v}{\rho_c}(W_0 + I_c^l)\right) \\ &\stackrel{(i)}{=} \exp\left\{-\frac{v}{\rho_c}(W_0 + I_c^l)\right\} = \exp\left\{-\frac{vW_0}{\rho_c}\right\} \mathcal{L}_{I_c^l}\left(\frac{v}{\rho_c}\right), \end{aligned} \quad (6)$$

where  $I_c^l$  is the interference from VUEs on channel  $l$  in reuse mode, (i) comes from  $h_c \sim \exp(1)$ , and  $\mathcal{L}_{I_c^l}(\cdot)$  denotes the Laplace transform of the interferences' PDF. Define  $s \triangleq v/\rho_c$  and let  $d_r$  be the distance from one VUE to another, then

$$\begin{aligned} \mathcal{L}_{I_c^l}(s) &= \mathbf{E}_{I_c^l}[e^{-sI_c^l}] = \mathbf{E}_{P_r, h_r, d_r}[e^{-s \sum_{X_i \in \Phi_r^l} P_r h_r d_r^{-\eta_r}}] \\ &= \prod_{X_i \in \Phi_r^l} \mathbf{E}_{P_r, h_r, d_r}[e^{-s P_r h_r d_r^{-\eta_r}}], \end{aligned}$$

where we denote  $\mathcal{X}_c \triangleq \{x, y, z | 0 < x \leq \frac{P_r}{\rho_c}, y \geq 0, L_0 \leq z \leq L_{\max}\}$  and  $\mathcal{X}'_c \triangleq \{x, z | 0 < x \leq \frac{P_r}{\rho_c}, L_0 \leq z \leq L_{\max}\}$ . Subsequently, we have

$$\begin{aligned} &\mathbf{E}_{P_r, h_r, d_r}[e^{-s P_r h_r d_r^{-\eta_r}}] \\ &= \iiint_{\mathcal{X}_c} e^{-sxy z^{-\eta_r}} f_{Reuse, tr}(x) e^{-y} f_{V2B}(z) dx dy dz \\ &= \iint_{\mathcal{X}'_c} \frac{4\beta z [L(\frac{x}{\rho_r})^{\frac{1}{\eta_r}-1} - (\frac{x}{\rho_r})^{\frac{2}{\eta_r}-1}]}{L^3 \eta_r \rho_r (1 + sxz^{-\eta_r}) \sqrt{z^2 - L_0^2}} dx dz \\ &\triangleq \iint_{\mathcal{X}'_c} f_{I_c^l}(x, z, v) dx dz. \end{aligned}$$

According to the independence between VUEs in reuse mode, we have

$$\begin{aligned}\mathcal{L}_{I_c^l}(s) &= \prod_{X_i \in \Phi_r^l} \mathbf{E}_{P_r, h_r, d_r} [e^{-s P_r h_r d_r^{-\eta_r}}] \\ &= \left( \iint_{\mathcal{X}'_c} f_{I_c^l}(x, z, v) dx dz \right)^{|\Phi_r^l|},\end{aligned}$$

where  $|\Phi_r^l| = N_r \mathcal{P}(d \leq D) x_r p_m p_l$  is the number of VUEs in reuse mode choosing channel  $l$ .

According to the Shannon's formula, we could calculate the average spectrum efficiency for cellular mode:

$$\begin{aligned}\bar{\tau}_c &= \mathbf{E} [\log_2(1 + \text{SINR}_c^l)] = \int_0^\infty \mathbb{P}(\text{SINR}_c^l > 2^t - 1) dt \\ &= \int_0^\infty p_c(\mathbf{x}, 2^t - 1) dt = \int_0^\infty \frac{1}{(v+1) \ln 2} p_c(\mathbf{x}, v) dv,\end{aligned}$$

where  $p_c(\mathbf{x}, v)$  represents coverage probability of a potential VUE in the cellular mode.

Note that, for cellular mode, the cellular BS scheduled the spectrum resources in a RR manner and the probability being allocated a subchannel  $l$  is  $1/E(N_{\text{Cellular}})$  for a VUE, where  $E(N_{\text{Cellular}})$  represents the mean number of VUEs in cellular mode. Thus, the average spectrum bandwidth allocated to a VUE under cellular mode is derived as follows:

$$B_c = \sum_{l=1}^F \frac{B}{E(N_{\text{Cellular}})} = \frac{FB}{N_r \mathbb{P}(d \geq D) + N_r \mathbb{P}(d \leq D) x_c}.$$

So the average transmission rate of a potential VUE choosing cellular mode is  $\tau_c = B_c \bar{\tau}_c$ .

### B. Average Transmission Rate of VUEs in Reuse Mode

Similarly, we first analyze the interference to calculate the SINR of VUEs in reuse mode, and then derive the average transmission rate according to the Shannon's formula.

When a potential VUE of reuse mode accesses subchannel  $l$ , the interference comes from the VUE of cellular mode choosing the same subchannel (denoted as  $I_{cr}^l$ ) and other VUEs of reuse mode reusing subchannel  $l$  (denoted as  $I_{rr}^l$ ). Then, the interference suffered by the receiver of reuse mode in channel  $l$  can be derived as follows:

$$I_r^l = I_{cr}^l + I_{rr}^l = P_c h_c d_r^{-\eta_c} + \sum_{X_i \in \Phi_{rr}^l} P_r h_r d_r^{-\eta_r}. \quad (7)$$

Correspondingly, we could derive the SINR of the reuse receiver as follows:

$$\text{SINR}_r^l = \frac{P_r h_r d_r^{-\eta_r}}{I_r^l + W_0} = \frac{\rho_r h_r}{I_r^l + W_0}, \quad (8)$$

where  $h_r$  is the fading gain from the transmitter to its receiver,  $d_r$  represents the distance between the tagged reuse transmitter and its receiver, and  $W_0$  represents noise power.

Using stochastic geometry tools, we derive the coverage probability  $p_r(\mathbf{x}, v)$  of a potential VUE in reuse mode as:

$$p_r(\mathbf{x}, v) = \mathbb{P}(\text{SINR}_r^l > v) = \mathbb{P}\left(h_r > \frac{v}{\rho_r} (W_0 + I_{cr}^l + I_{rr}^l)\right)$$

$$\begin{aligned}&\stackrel{(i)}{=} \exp\left\{-\frac{v}{\rho_r} (W_0 + I_{cr}^l + I_{rr}^l)\right\} \\ &= \exp\left\{-\frac{v W_0}{\rho_r}\right\} \mathcal{L}_{I_{cr}^l}\left(\frac{v}{\rho_r}\right) \mathcal{L}_{I_{rr}^l}\left(\frac{v}{\rho_r}\right),\end{aligned} \quad (9)$$

where  $I_{cr}^l$  and  $I_{rr}^l$  represent the interferences from VUEs on channel  $l$  in cellular mode and reuse mode respectively, (i) follows that  $h_r \sim \exp(1)$ . Denote  $s_r \triangleq v/\rho_r$ , we have

$$\mathcal{L}_{I_{cr}^l}(s_r) = \mathbf{E}_{I_{cr}^l} [e^{-s_r I_{cr}^l}] = \mathbf{E}_{P_c, h_c, d_r} [e^{-s_r P_c h_c d_r^{-\eta_c}}].$$

We denote  $\mathcal{Y}_c \triangleq \{x, y, z \mid \rho_c L_0^{\eta_c} \leq x \leq \rho_c L_{\max}^{\eta_c}, y \geq 0, 0 < z \leq L\}$  and  $\mathcal{Y}'_c \triangleq \{x, z \mid \rho_c L_0^{\eta_c} \leq x \leq \rho_c L_{\max}^{\eta_c}, 0 < z \leq L\}$ , then

$$\begin{aligned}\mathcal{L}_{I_{cr}^l}(s_r) &= \mathbf{E}_{P_c, h_c, d_r} [e^{-s_r P_c h_c d_r^{-\eta_c}}] \\ &= \iiint_{\mathcal{Y}_c} e^{-s_r x y z^{-\eta_c}} f_{\text{Cellular}, tr}(x) e^{-y} f_{V2V}(z) dx dy dz \\ &= \iint_{\mathcal{Y}'_c} \frac{4 \rho_c^{-\frac{2}{\eta_c}} x^{\frac{2}{\eta_c}-1} (L-z)}{L^3 \eta_c (1 + s_r x z^{-\eta_c}) \sqrt{\left(\frac{x}{\rho_c}\right)^{\frac{2}{\eta_c}} - L_0^2}} dx dz \\ &\triangleq \iint_{\mathcal{Y}'_c} f_{I_{cd}^l}(x, z, v) dx dz.\end{aligned}$$

For  $\mathcal{L}_{I_{rr}^l}(s_r)$ , we can derive it as follows:

$$\begin{aligned}\mathcal{L}_{I_{rr}^l}(s_r) &= \mathbf{E}_{I_{rr}^l} [e^{-s_r I_{rr}^l}] = \mathbf{E}_{P_r, h_r, d_r} [e^{-s_r \sum_{X_i \in \Phi_{rr}^l} P_r h_r d_r^{-\eta_r}}] \\ &= \prod_{X_i \in \Phi_{rr}^l} \mathbf{E}_{P_r, h_r, d_r} [e^{-s_r P_r h_r d_r^{-\eta_r}}].\end{aligned}$$

We denote  $\mathcal{Z}_c \triangleq \{x, y, z \mid 0 < x \leq P_r^{\max}, y \geq 0, 0 < z \leq L\}$  and  $\mathcal{Z}'_c \triangleq \{x, z \mid 0 < x \leq P_r^{\max}, 0 < z \leq L\}$ , then

$$\begin{aligned}\mathbf{E}_{P_r, h_r, d_r} [e^{-s_r P_r h_r d_r^{-\eta_r}}] &= \iiint_{\mathcal{Z}_c} e^{-s_r x y z^{-\eta_r}} f_{\text{Reuse}, tr}(x) e^{-y} f_{V2V}(z) dx dy dz \\ &= \iint_{\mathcal{Z}'_c} \frac{4 \beta (L-z) \left[ L \left(\frac{x}{\rho_r}\right)^{\frac{1}{\eta_r}-1} - \left(\frac{x}{\rho_r}\right)^{\frac{2}{\eta_r}-1} \right]}{L^4 \eta_r \rho_r (1 + s_r x z^{-\eta_r})} dx dz \\ &\triangleq \iint_{\mathcal{Z}'_c} f_{I_{rr}^l}(x, z, v) dx dz.\end{aligned}$$

According to the independence between VUEs in reuse mode, we have

$$\begin{aligned}\mathcal{L}_{I_{rr}^l}(s_r) &= \prod_{X_i \in \Phi_{rr}^l} \mathbf{E}_{P_r, h_r, d_r} [e^{-s_r P_r h_r d_r^{-\eta_r}}] \\ &= \left( \iint_{\mathcal{Z}'_c} f_{I_{rr}^l}(x, z, v) dx dz \right)^{|\Phi_{rr}^l|},\end{aligned}$$

where  $|\Phi_{rr}^l| = |\Phi_r^l| - 1 = \max\{N_r \mathcal{P}(d \leq D) x_d p_m p_l - 1, 0\}$  represents the number of other interferers VUE pairs choosing channel  $l$  in reuse mode.

According to the Shannon's formula, we could derive the average spectrum efficiency of a potential VUE when transmitting

in reuse mode as follows:

$$\begin{aligned}\bar{\tau}_r &= \mathbf{E} [\log_2(1 + \text{SINR}_r^l)] = \int_0^\infty \mathbb{P} [\text{SINR}_r^l > 2^t - 1] dt \\ &= \int_0^\infty p_r(\mathbf{x}, 2^t - 1) dt = \int_0^\infty \frac{1}{(v+1) \ln 2} p_r(\mathbf{x}, v) dv,\end{aligned}$$

where  $p_r(\cdot)$ , as in (9), represents a potential VUE's coverage probability in reuse mode.

According to the spectrum allocation schemes, the average bandwidth allocated to a VUE in reuse mode is  $B_r = k p_m B$ . Hence, the average transmission rate of a potential VUE accessing reuse mode is derived as  $\tau_r = B_r \bar{\tau}_r = k p_m B \bar{\tau}_r$ .

### C. Average Transmission Rate of VUEs in Dedicated Mode

Here, the performance analysis of dedicated data pipe is considered to apply IEEE 802.11 DCF basic access scheme [31]. Assume that there are  $N_{Dedicated}$  VUEs choosing the dedicated mode (forming the dedicated mode set  $N_d$ ), we focus on the vehicular transmission between a given pair of VUEs, i.e., VUE  $i$  and VUE  $j$ , where each packet is transmitted using the CSMA/CA scheme. The contention window size  $CW$  is used for counting the backoff time. For each VUE in dedicated mode, we denote  $\varsigma$  as the average transmission probability, then  $\varsigma = 2/(CW + 1)$ . Let  $p_{suc}$  be the probability that any single VUE within the carrier sensing range transmits messages on the specific spectrum successfully in the considered slot, and  $p_{suc} = N_{Dedicated} \times \varsigma(1 - \varsigma)^{N_{Dedicated} - 1}$ . Denote  $p_{tr}$  as the probability of at least one transmission within the considered slot duration, then  $p_{tr} = 1 - (1 - \varsigma)^{N_{Dedicated}}$ . We denote  $T_e$ ,  $T_s$ , and  $T_c$  as the duration time of an empty slot, the average busy time of sensory channel, and the average busy time of each VUE sensing channel in a collision, respectively. In IEEE 802.11 standard,  $T_e = \sigma$ , and for a basic access scheme, the successful frame transmission  $T_s$  and the collided transmission time  $T_c$  could be given as follows:

$$\begin{cases} T_s = H + E[P] + SIFS + 2\sigma + ACK + DIFS, \\ T_c = H + E[P^*] + SIFS + DIFS + \sigma, \end{cases} \quad (10)$$

where  $H = PHY_{hdr} + MAC_{hdr}$  represents the package header size and consists of medium access control (MAC) header and physical layer (PHY) header,  $E[P^*]$  denotes the average length of the biggest packet payload in a collision,  $SIFS$  is a period of time equal to a Short inter-frame space (SIFS),  $ACK$  is the time of acknowledgement and  $DIFS$  is a period of time equal to a distributed inter-frame space (DIFS).

Introducing the conclusions in [31], we could evaluate the MAC transmission throughput  $T_{N_d}^j$  of dedicated data pipe applying CSMA/CA protocol within the carrier sensing range of VUE  $j$ ,  $j \in N_d$ . First,  $T_{N_d}^j$  is defined as the fraction of time the channel is used to successfully transmit payload bits, which can be expressed as the ratio:

$$T_{N_d}^j = \frac{E[\text{payload information transmitted in a slot time}]}{E[\text{length of a slot time}]} \quad (11)$$

Let  $P_j$  represents the packet payload size of VUE  $j$ , the average amount of payload information successfully transmitted in a slot time is  $\varsigma p_{suc} P_j$ . The average length of a slot time consists of the following parts. With probability  $1 - \varsigma$ , the slot time is empty, it contains a successful transmission with probability  $\varsigma p_{suc}$ , and it contains a collision with probability  $\varsigma(1 - p_{suc})$ . Hence, (11) becomes the following expression:

$$T_{N_d}^j = \frac{\varsigma p_{suc} P_j}{(1 - p_{tr})\sigma + p_{suc} T_s + (p_{tr} - p_{suc}) T_c} \quad (12)$$

Then, we can calculate the mean MAC transmission throughput  $\text{THR}_{N_d}^j$  if VUE  $j$  applies the dedicated data pipe, which is expressed as follow:

$$\text{THR}_{N_d}^j = \sum_{j \in N_d} T_{N_d}^j / N_{Dedicated} \quad (13)$$

We can see that the throughput of dedicated mode just relies on the number of VUEs in this mode and their packet sizes. Therefore, if the packet sizes are all the same for VUEs, the average transmission rate of dedicated mode is  $\tau_d = T_{N_d}^j$ .

## V. EVOLUTIONARY GAME OF MULTI-MODE SELECTION IN 5G-VANET

In this section, we first introduce the evolutionary game for VUEs and describe the game process. Then, we use replicator dynamics to analyze the interaction between the dynamic pricing and the distribution of VUEs. Finally, we propose a three-mode selection algorithm based on the evolutionary game, which relies on the dynamic pricing of the cellular BS.

### A. Description of Proposed Evolutionary Game Model

Considering the bounded rationality of VUEs, we use the evolutionary game to model the adaptive mode selection of VUEs as follows.

- *Player*: The potential VUEs act as the players in the evolutionary game.
- *Strategy*: The strategy is the selected communication mode. Hence, the set of possible strategies for each player is  $\mathcal{M} = \{c, r, d\}$ , where  $c$ ,  $r$  and  $d$  represents the cellular mode, reuse mode and dedicated mode, respectively.
- *Population*: VUEs selecting the same communication mode form a population. That is, the population for strategy  $i \in \mathcal{M}$  is the number of VUEs in mode  $i$ .
- *Population share*: The population share for strategy  $i \in \mathcal{M}$  is defined as  $x_i = n_i/N$ , where  $n_i$  and  $N$  represent the number of VUEs selecting strategy  $i$  and total population, respectively.
- *Population profile*: With the population share for each mode, we denote the population profile as the vector  $\mathbf{x} = [x_c, x_r, x_d]^T \in \mathcal{X}$ , where  $\mathcal{X} \triangleq \{\mathbf{x} \in \mathbb{R}^3 | x_i \in [0, 1], \sum_{i \in \mathcal{M}} x_i = 1\}$  represents the set of all possible population profiles.
- *Access prices*: To show the impact of prices on the three modes, we normalize the access prices as a vector  $\mathbf{p} = [p_c, p_r, p_d]^T \in \mathcal{P}$ , where  $\mathcal{P} \triangleq \{\mathbf{p} \in \mathbb{R}^3 | p_i \in [0, 1], \sum_{i \in \mathcal{M}} p_i = 1\}$ .



- *Payoff*: The payoff function of a potential VUE in mode  $i \in \mathcal{M}$  is defined as:

$$\pi(i, \mathbf{x}, \mathbf{p}) = \varpi(\tau_i(\mathbf{x})) - p_i, \quad (14)$$

where  $\varpi(\tau_i(\mathbf{x}))$  is the utility function of achieved transmission rate. Here, we simply use a linear function to quantify the rate utility as  $\varpi(\tau_i(\mathbf{x})) = \alpha \tau_i(\mathbf{x})$ , where  $\alpha = 1/\|\tau(\mathbf{x})\|_1$  is a normalized coefficient and  $\tau(\mathbf{x}) = [\tau_c(\mathbf{x}), \tau_r(\mathbf{x}), \tau_d(\mathbf{x})]^T$  represents the average transmission rate of each mode.

- *Average payoff*: With the population profile  $\mathbf{x}$  and payoff of VUEs in different modes in (14), we define the average payoff as  $\pi(\mathbf{x}, \mathbf{x}, \mathbf{p}) = \sum_{i \in \mathcal{M}} x_i \pi(i, \mathbf{x}, \mathbf{p})$ , where  $x_i$  is the population share of strategy  $i \in \mathcal{M}$ .

### B. Evolutionary Stable Strategy

The evolutionary stable strategy (ESS) is a very important concept in the evolutionary game. We assume that some VUEs change their mode strategies, called as the mutants of the population. Let  $\varepsilon \in (0, 1)$  be the size of mutants after normalization and their population profile is denoted as  $\mathbf{x}'$ . Then, the population profile after mutation can be denoted as  $(1 - \varepsilon)\mathbf{x} + \varepsilon\mathbf{x}'$ . After mutation, the average payoff of non-mutants and mutants are denoted as  $\pi(\mathbf{x}, (1 - \varepsilon)\mathbf{x} + \varepsilon\mathbf{x}', \mathbf{p})$  and  $\pi(\mathbf{x}', (1 - \varepsilon)\mathbf{x} + \varepsilon\mathbf{x}', \mathbf{p})$ , respectively. We define the evolutionary stable strategy as follows.

*Definition (ESS)*: A strategy  $\mathbf{x}$  is an ESS, if  $\forall \mathbf{x}' \neq \mathbf{x}, \exists \varepsilon_{\mathbf{x}'} \in (0, 1)$  such that:  $\forall \varepsilon \in (0, \varepsilon_{\mathbf{x}'})$ ,

$$\pi(\mathbf{x}, (1 - \varepsilon)\mathbf{x} + \varepsilon\mathbf{x}', \mathbf{p}) > \pi(\mathbf{x}', (1 - \varepsilon)\mathbf{x} + \varepsilon\mathbf{x}', \mathbf{p}). \quad (15)$$

That is, after mutation, non-mutants (i.e., VUEs that keep their strategy unchanged) can achieve the larger average utility than mutants (i.e., VUEs that change their strategy).

Notice that, an ESS is also a Nash equilibrium (NE), because the ESS is also the best strategy to itself. Once an ESS is reached, the system is stable. At the same time, the ESS's evolutionary stability also provides a great refinement for the NE. Unlike the NE where a single player would not benefit through making a unilateral change of strategy, the ESS could avoid the mutant for a group of players. We consider an ESS as the supposed solution of VUEs' three-mode selection.

### C. Replicator Dynamics of Three-Mode Selection Evolution

In the process of followers' evolutionary game, each potential VUE would adaptively adjust the mode selection strategy, which leads to a better payoff than the average. After this, the other VUEs could learn and replicate the mode selection strategies. In this way, the population share and the population profile would be changed through the adaptive mode selection strategies of VUEs, that is, evolve over time. Hence, we denote population share  $x_i(t)$  and population profile  $\mathbf{x}(t)$  as a function of time  $t$ , respectively. According to [27], the evolution of population profile is governed by the replicator dynamics:

$$\dot{x}_i(t) = \delta x_i(t) [\pi(i, \mathbf{x}(t), \mathbf{p}(t)) - \pi(\mathbf{x}(t), \mathbf{x}(t), \mathbf{p}(t))], \quad (16)$$

in which  $\delta$  represents the learning rate of evolutionary dynamics and controls the frequency of the three-mode selection adaptation [32]. As we can see, if the corresponding payoff is higher than the average in some  $t$ , i.e.,  $\pi(i, \mathbf{x}(t), \mathbf{p}(t)) > \pi(\mathbf{x}(t), \mathbf{x}(t), \mathbf{p}(t))$ , the number of potential VUEs choosing mode  $i \in \mathcal{M}$  would increase, i.e.,  $\dot{x}_i(t) > 0$ . It is easy to see that the replicator dynamics must guarantee that  $x_i(t)$  always lies in  $[0, 1]$  during the evolution which would be proved in the following Lemma 1.

*Lemma 1*: The population shares can guarantee evolutionary requirements, i.e.,  $\sum_{i \in \mathcal{M}} x_i(t) = 1$  and  $x_i(t) \in [0, 1], \forall t \in [0, \infty)$ , during the mode selection.

*Proof*: With initial state  $\sum_{i \in \mathcal{M}} x_i(0) = 1$  and definition  $\pi(\mathbf{x}(t), \mathbf{x}(t), \mathbf{p}(t)) = \sum_{i \in \mathcal{M}} \pi(i, \mathbf{x}(t), \mathbf{p}(t))$ , we have the replicator dynamics (16) of the initial state:

$$\begin{aligned} \sum_{i \in \mathcal{M}} \dot{x}_i(0) &= \sum_{i \in \mathcal{M}} \delta x_i(0) [\pi(i, \mathbf{x}(0), \mathbf{p}(0)) - \pi(\mathbf{x}(0), \mathbf{x}(0), \mathbf{p}(0))] \\ &= \delta \pi(\mathbf{x}(0), \mathbf{x}(0), \mathbf{p}(0)) - \delta \pi(\mathbf{x}(0), \mathbf{x}(0), \mathbf{p}(0)) = 0. \end{aligned}$$

Then, after an evolution time  $t$  from initial state, the population distribution becomes the following expression:  $x_i(t) = x_i(0) + t \dot{x}_i(0)$  and

$$\sum_{i \in \mathcal{M}} x_i(t) = \sum_{i \in \mathcal{M}} x_i(0) + t \sum_{i \in \mathcal{M}} \dot{x}_i(0) = 1.$$

Hence, we have the summation of the variation rate:

$$\begin{aligned} \sum_{i \in \mathcal{M}} \dot{x}_i(t) &= \sum_{i \in \mathcal{M}} \delta x_i(t) [\pi(i, \mathbf{x}(t), \mathbf{p}(t)) - \pi(\mathbf{x}(t), \mathbf{x}(t), \mathbf{p}(t))] \\ &= \delta \pi(\mathbf{x}(t), \mathbf{x}(t), \mathbf{p}(t)) - \delta \pi(\mathbf{x}(t), \mathbf{x}(t), \mathbf{p}(t)) = 0. \end{aligned}$$

It shows that the sum of population shares is independent of time and does not vary over time.

According to the replicator dynamics (16), we have  $\dot{x}_i(t) \geq 0$  with  $x_i(t) = 0$ . Also, when  $x_i(t) = 1$ ,  $\pi(i, \mathbf{x}(t), \mathbf{p}(t)) = \pi(\mathbf{x}(t), \mathbf{x}(t), \mathbf{p}(t))$  holds true, which implies  $\dot{x}_i(t) \leq 0$  with  $x_i(t) = 1$ . Therefore, if  $x_i(t) \rightarrow 0$  or  $1$ , it holds  $\dot{x}_i(t) \rightarrow 0$ , which results in  $x_i(t) \in [0, 1], \forall t \in [0, \infty)$ . ■

On basis of Lemma 1, we can see that there is a dependency between the three-mode selection strategies of potential VUEs and the prices of the cellular BS. The following Theorem 1 will discuss the existence and uniqueness of the solution for the mode selection replicator dynamics, which is regarded as the termination condition of the Algorithm 1.

*Theorem 1*: For differential equations denoted in (16) with  $\mathbf{x}(0) = \mathbf{x}_0$ , if  $\mathbf{p}(t)$  is measurable for  $t \in [0, \infty)$ , there exists a unique solution  $\mathbf{x}(t), t \in [0, \infty)$  for  $\dot{x}_i(t) = 0$ .

*Proof*: According to replicator dynamics (16), we denote  $\dot{x}_i(t) = f_i(t, \mathbf{x}(t), \mathbf{p}(t))$  and  $\mathbf{x}(0) = \mathbf{x}_0$ . When  $t$  is fixed, the partial derivative  $\frac{\partial f_i(t, \mathbf{x}(t), \mathbf{p}(t))}{\partial \mathbf{x}(t)}$  is continuous, due to the analytic expressions of  $\dot{x}_i(t)$  and  $\pi(\cdot)$  in Section IV. If  $\mathbf{p}(t)$  is measured for any  $t \in [0, \infty)$ , then  $f_i(t, \mathbf{x}(t), \mathbf{p}(t))$  would be a measurable function for fixed  $x_i(t)$  on  $t \in [0, \infty)$ . Furthermore, since the achievable rate and prices are bounded,  $f_i(t, \mathbf{x}(t), \mathbf{p}(t))$  is also



bounded. Combining the continuity and boundedness of function  $f_i(t, \mathbf{x}(t), \mathbf{p}(t))$  in regard to  $\mathbf{x}(t)$ , we derive that gradient  $\frac{\partial f_i(t, \mathbf{x}(t), \mathbf{p}(t))}{\partial \mathbf{x}(t)}$  has an upper limit  $Q$ .

Hence, according to the definition of gradient, it yields that  $|f_i(t, \mathbf{x}(t), \mathbf{p}(t)) - f_i(t, \mathbf{y}(t), \mathbf{x}(t))| \leq Q|\mathbf{x}(t) - \mathbf{p}(t)|$  for any population profile  $\mathbf{x}$  and  $\mathbf{y}$ , which implies that  $Q$  is the Lipschitz constant and  $f_i(\mathbf{x}(t), \mathbf{p}(t))$  satisfies the global Lipschitz condition. Denote  $\varphi_0(t) = \mathbf{x}_0$  and  $\varphi_{k+1}(t) = \mathbf{x}_0 + \int_{t_0}^t f_i(s, \mathbf{x}(s), \mathbf{p}(s)) ds$ . It can then be shown that, by using the Banach fixed point theorem [33], the sequence of Picard iterates  $\varphi_k$  is convergent and the limit is the solution. According to the above, we conclude that there exists globally a unique solution for these differential equations. ■

#### D. EE and ESS Solutions of the Evolutionary Game

An evolutionary equilibrium (EE) is regarded as the equilibrium state, where all potential VUEs have no motivation to change their strategies. Subsequently, we could obtain the EE by solving the equations:  $\dot{x}_i(t) = 0, \forall i \in \mathcal{M}$ . At equilibrium state, all potential VUEs achieve the average payoff, which guarantees fairness among them. According to the replicator dynamics (16), there exist boundary EE and interior EE. The boundary EE means that there exists a population share  $x_i = 1$  and  $x_j = 0, \forall j \neq i \in \mathcal{M}$ , while the interior EE  $\tilde{\mathbf{x}}$  satisfies  $\tilde{x}_i \in (0, 1), \forall i \in \mathcal{M}$ . The boundary EE is not robust because any small perturbation would deviate the population share from the EE. Hence, the boundary EE fails to be the expected ESS. In order to prove the robustness of the interior EE, we need to evaluate the eigenvalues of the Jacobian matrix of the replicator dynamics (16). If these eigenvalues all have a negative real part, the interior EE is stable. Due to the complexity of the expressions for the transmission rates, it is almost impossible to analytically solve the eigenvalues for the replicator dynamics. Instead, we plot the direction field of followers' replicator dynamics in simulations (Fig. 8), which demonstrates the stability and convergence of the interior EE. Hence, for the proposed evolutionary game, the interior EE becomes an ESS. The benefits of ESS are stability, fairness, and performance optimization. Our goal is to allow VUEs to reach their ESS by dynamically adjusting their strategies. The detailed evolutionary process to achieve ESS is shown in Algorithm 1, where the decision time  $T$  is equally divided into  $n$  decision points (line 3). In the decision points, the potential VUEs would adaptively choose their strategies according to the evolutionary game rule, i.e., imitate the strategy with higher payoff (lines 4-6).

### VI. DYNAMIC PRICING OF THE CELLULAR BS

In this section, we first model the dynamic pricing problem for cellular BS as a leader control. Then, a discretization method is proposed to solve the dynamic pricing problem.

#### A. Dynamic Pricing as the Leader Control

The leader control strategy is considered to be an open-loop structure, which does not require any feedback. Under the open-loop structure, cellular BS decides the control strategy

---

#### Algorithm 1: VUEs-Controlled Mode Selection Algorithm.

---

- 1: The cellular BS uses an open-loop strategy to calculate the dynamic pricing in advance.
  - 2: Each VUE randomly chooses a communication mode  $i \in \mathcal{M}$ , measures its achieved rate and sent it to the BS including the selected mode.
  - 3: **for**  $j = 1$  to  $n$  (assume there are  $n$  decision points in duration time  $T$ ) **do**
  - 4: The BS collects the mode selection and rate information from all VUEs, calculates the normalized coefficient  $\alpha$ , average payoff  $\pi_j(\mathbf{x}_j, \mathbf{x}_j, \mathbf{p}_j)$  and broadcasts them with the access prices  $\mathbf{p}_j$  to all VUEs.
  - 5: For each VUE, it first calculates its payoff  $\pi_j(i, \mathbf{x}_j, \mathbf{p}_j)$  according to (14) and makes the following mode selection: if its payoff is less than average payoff, i.e.,  $\pi_j(i, \mathbf{x}_j, \mathbf{p}_j) < \pi_j(\mathbf{x}_j, \mathbf{x}_j, \mathbf{p}_j)$ , it randomly selects another mode  $i'$  with higher payoff than average payoff (if there exists), i.e.,  $\pi_j(i', \mathbf{x}_j, \mathbf{p}_j) \geq \pi_j(\mathbf{x}_j, \mathbf{x}_j, \mathbf{p}_j)$ , else it remains unchanged.
  - 6: Each VUE measures its transmission rate and sends it to the BS including its communication mode.
  - 7: The steps from 4 to 6 are repeated until no VUE changes its mode or the time is out.
  - 8: **end for**
- 

ahead of time and carries out the strategy throughout the process. The open-loop strategy space set could be denoted as  $\mathcal{P} = \{\mathbf{p}(t) | \mathbf{e}^T \mathbf{p}(t) = 1, \mathbf{p}(t) \geq 0, \forall t \in [0, T]\}$ ,  $\mathbf{e} \triangleq [1, 1, 1]^T$ .

The cellular BS aims at maximizing its revenue which is defined as the sum of access price paid by all VUEs:

$$U(\mathbf{x}(t), \mathbf{p}(t)) = \sum_{i \in \mathcal{M}} N x_i(t) p_i(t),$$

where  $N$  represents the number of total VUEs,  $\mathbf{x}(t)$  and  $\mathbf{p}(t)$  represents the population profile of VUEs and access prices for different communication modes, respectively.

In order to optimize the performance of 5G-VANET, we also try to induce VUEs' distribution close to a pre-optimized one. Here, we use the maximization of sum-rate as the optimal system performance criteria. Especially, given 5G-VANET parameters, we could derive the average rate of each mode  $\tau_c, \tau_d, \tau_d$  according to Section IV. Then, we could get the optimal population profile  $\mathbf{x}^*$  from the following problems:

$$\begin{aligned} \max_{\mathbf{x}} \quad & [\tau_c, \tau_d, \tau_d] \cdot N \cdot \mathbf{x} \\ \text{s.t.} \quad & \mathbf{e}^T \mathbf{x} = 1, \quad 0 \leq \mathbf{x} \leq \mathbf{e}, \end{aligned} \quad (17)$$

where  $N = N_r \mathcal{P}(d \leq D)$  is the number of potential VUEs and  $\mathbf{x} = [x_c, x_d, x_d]^T$  is the population profile which gives the fraction of VUEs selecting each mode. Considering that the constraint set of the problem (17) is linear, the interior point method could be introduced to efficiently solve the problem, which has an iteration complexity  $\mathcal{O}(n)$  [34].

As often used in the control theory, we introduce a performance cost function to formulate the performance discrepancy with optimal VUEs' population profile as follows:

$$C(\mathbf{x}(t), \mathbf{p}(t)) = \|\mathbf{x}(t) - \mathbf{x}^*\|^2,$$

where  $\mathbf{x}^*$  is the solution of problem (17). Then, we can denote the instantaneous profit of the cellular BS as the difference between its revenue and its performance cost:

$$\mathcal{U}(\mathbf{x}(t), \mathbf{p}(t)) = w_u U(\mathbf{x}(t), \mathbf{p}(t)) - w_c C(\mathbf{x}(t), \mathbf{p}(t)),$$

where  $w_u$  and  $w_c$ , satisfying  $w_u + w_c = 1$ ,  $w_u, w_c \in [0, 1]$ , represent the weighting factors.

Using the open-loop strategy, leader control strategy, and the instantaneous profit, we formulate the leader control problem as follows, which is the dynamic pricing of the cellular BS.

$$\begin{aligned} & \max_{\mathbf{p}(t)} \int_0^T e^{-\rho t} \mathcal{U}(\mathbf{x}(t), \mathbf{p}(t)) dt \\ & \text{s.t. } \dot{x}_i(t) = \delta x_i(t) [\pi(i, \mathbf{x}(t), \mathbf{p}(t)) - \pi(\mathbf{x}(t), \mathbf{x}(t), \mathbf{p}(t))], \\ & \quad \mathbf{x}(0) = \mathbf{x}_0, \mathbf{p}(t) \in \mathcal{P}, i \in \{c, r, d\}, \end{aligned} \quad (18)$$

where  $\rho$  is a discount factor representing the influence of time on future payoff,  $\pi(i, \mathbf{x}(t), \mathbf{p}(t))$  is the payoff of each VUE and  $\pi(\mathbf{x}(t), \mathbf{x}(t), \mathbf{p}(t))$  is their average payoff.

### B. The Discretization Method

In this section, we propose a discretization method to solve the dynamic pricing problem (18) of the cellular BS. The time period  $[0, T]$  is discretized into  $L$  decision points and unit time  $h = T/L$ . By defining  $F(t) \triangleq e^{-\rho t} \mathcal{U}(\mathbf{x}(t), \mathbf{p}(t))$  and using Riemann integral [35], we can approximate the objective function  $\int_0^T F(t) dt$  in problem (18) as  $\sum_{k=1}^L h \cdot F(kh)$ .

With the approximations  $\mathbf{x}(kh) = \mathbf{x}^k$  and  $\mathbf{p}(kh) = \mathbf{p}^k$  (the population profile and access prices in  $k$ -th decision point, respectively), the optimal control problem (18) can be transformed into the following nonlinear program (NLP):

$$\begin{aligned} & \max \sum_{k=1}^L h \cdot F(kh) \\ & \text{s.t. } \mathbf{x}^{k+1} = \mathbf{x}^k + h \cdot \delta \mathbf{x}_k [\pi(\mathbf{x}^k, \mathbf{p}^k) - \bar{\pi}(\mathbf{x}^k, \mathbf{p}^k)], \end{aligned} \quad (19)$$

for  $k \in \{1, \dots, L\}$ . The optimization variable is represented by the vector  $\mathbf{v} = [\mathbf{p}^0, \mathbf{x}^0, \dots, \mathbf{p}^{L-1}, \mathbf{x}^{L-1}, \mathbf{x}^L]$ .

The Lagrange function for the NLP is given by:

$$\begin{aligned} L(\mathbf{v}, \beta) = & \sum_{k=1}^L h \cdot F(kh) + \sum_{k=1}^L \beta (x^{k+1} - \mathbf{x}^k \\ & - h \cdot \delta \mathbf{x}^k [\pi(\mathbf{x}^k, \mathbf{p}^k) - \bar{\pi}(\mathbf{x}^k, \mathbf{p}^k)]). \end{aligned}$$

The Karush-Kuhn-Tucker (KKT) optimality conditions for the NLP are given by  $\frac{\partial L(\mathbf{v}, \beta)}{\partial \mathbf{x}^k} = 0$  and  $\frac{\partial L(\mathbf{v}, \beta)}{\partial \mathbf{p}^k} = 0$ . Numerical methods, such as interior point method [34], can be used to solve the above NLP and obtain the optimal dynamic pricing.

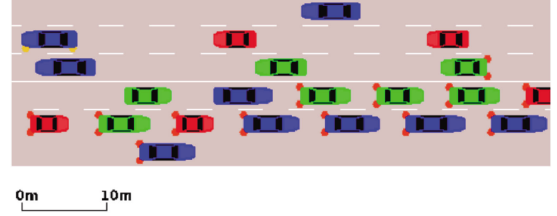


Fig. 3. A snapshot of the generated traffic scenario in SUMO.

TABLE III  
SIMULATION PARAMETERS IN DEDICATED MODE

Parameters	Value	Parameters	Value
CW	32	ACK	240 $\mu$ s
SIFS	28 $\mu$ s	DIFS	128 $\mu$ s
Packet payload	8184 bits	$\sigma$	50 $\mu$
MAC header	272 bits	PHY header	128 bits

## VII. NUMERICAL ANALYSIS

In this section, we elaborate on the simulation setting and present various simulation results to evaluate the effectiveness of the proposed framework. In addition, we show the influences of delay and dynamic pricing control on our framework.

### A. Simulation Parameters Setting

As shown in Fig. 3, we use Simulation of Urban Mobility (SUMO) [36] to generate various traffic flows with different densities, in which SUMO is used worldwide and is an open source, highly portable, microscopic and continuous road traffic simulation tool. We can set parameters, such as the number of vehicles, speed, and the road topology to generate traffic flows, and then get the distance between the vehicles. In the simulation setup, we set the range of the cellular BS as  $L = 1000$  m. The shortest distance from the BS to the highway is  $L_0 = 34$  m. We set the channel inversion threshold of cellular and reuse mode as  $\rho_c = -80$  dBm and  $\rho_d = -70$  dBm, respectively. The noise power  $W_0 = -90$  dBm, path-loss exponents  $\gamma_c = 3$ ,  $\gamma_d = 4$ , and the channel gain  $h \sim \exp(1)$ . The number of subchannels  $F = 20$ , each of which has a bandwidth  $B = 1$  MHz. The transmission rate of dedicated mode is 20 Mbps and the simulation parameters in dedicated mode is shown in Table III [5]. For reuse mode, each VUE randomly selects 6 subchannels as candidates (i.e.,  $k = 6$ ) and medium access probability  $p_m = 0.5$ . The maximum transmission power of VUEs in reuse mode  $P_r^{\max} = 200$  mW. According to the channel inversion power control model, the transmission distance threshold  $D = 211$  m and the probability  $\mathbb{P}(d \leq D) = 0.38$  for reuse mode. In the initial state, the potential VUEs select three communication modes with the same probability.

### B. Numerical Results

1) *Total Transmission Rates of VUEs Under Different Traffic Flows:* To evaluate the performance of multi-mode spectrum sharing in 5G-VANET, we compare the proposed Stackelberg pricing game algorithm with four benchmark schemes: only cellular mode, only reuse mode, only dedicated mode, and random

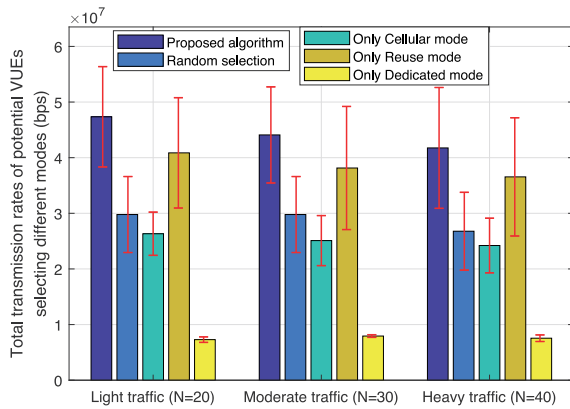


Fig. 4. Total transmission rates of potential VUEs in different modes (bps).

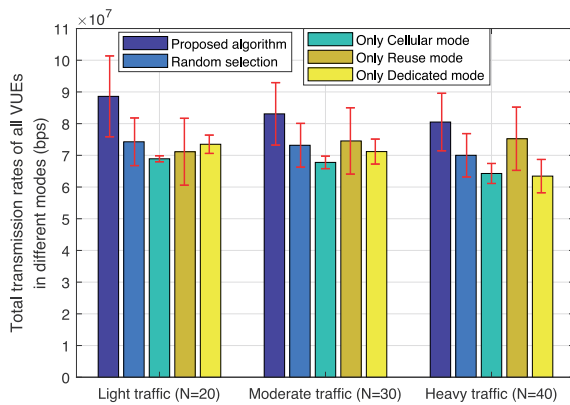


Fig. 5. Total transmission rates of all VUEs in different modes (bps).

selection. We use SUMO to generate 100 traffic flows under three traffic scenarios, i.e., light traffic ( $N = 20$ ), moderate traffic ( $N = 30$ ), heavy traffic ( $N = 40$ ), where  $N$  is the number of potential VUEs. Figs. 4 and 5 show total transmission rates of potential VUEs and all VUEs, respectively. In the figures, the bars are the average values, and the red line segments represent the confidence intervals of the results. It is observed that the proposed algorithm can significantly improve the total transmission rates of VUEs. Specifically, the proposed algorithm can improve the total transmission rates of potential VUEs by 500% and 60% compared with the only dedicated mode and random selection in light traffic scenario, respectively.

2) *Population Profile Evolution of Three-Mode Selection*: We first plot the population profile evolution of the three-mode selection under the replicator dynamics in (16) from the initial distribution to show the iterative process of the proposed algorithm. Figs. 6 and 7 show the evolution of proportions of potential VUEs and all VUEs in each mode, respectively. From Fig. 6, it is observed that the proportions of potential VUEs in all modes are convergent to the optimal population share, where no VUE has the willingness to churn. Meanwhile, it could be observed that the proportion of potential VUEs in cellular mode rapidly reduces to a small value. The reason is that there are already many VUEs forced to choose the cellular mode due to the transmission distance limit as shown in Fig. 7. If the proportion of VUEs in cellular mode continues to increase, it would result

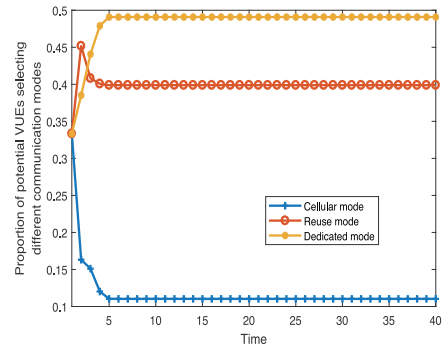


Fig. 6. Proportion of potential VUEs throughout the mode selection.

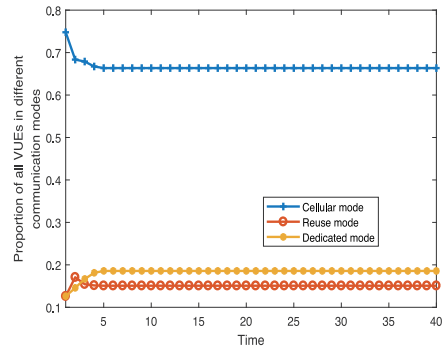


Fig. 7. Proportion of all VUEs throughout the mode selection.

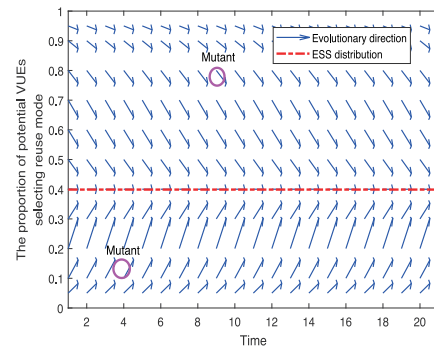


Fig. 8. Direction field of the replicator dynamics.

in a sharp decline in the average available bandwidth allocated to VUEs in cellular mode. Furthermore, it would seriously affect the overall transmission rate of the cellular mode. Therefore, for the potential VUEs, we can see that the strategy of choosing cellular mode is dominated by those of choosing the reuse and dedicated modes.

3) *Convergence of Population Shares*: We utilize a direction field of the replicator dynamics (16) in the evolutionary game to demonstrate the global convergence of the proposed algorithm. Fig. 8 shows the population share evaluation of VUEs selecting reuse mode. It can be seen that the population share could converge to ESS from any given inner initial point. Moreover, the convergence from any initial population share over time implies that the mutants could be eliminated during the three-mode selection process. That is, it further demonstrates the robustness



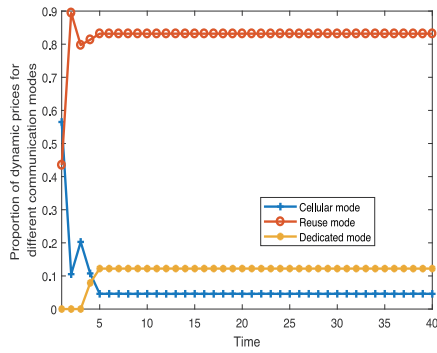


Fig. 9. Dynamic pricing control strategy of the cellular BS.

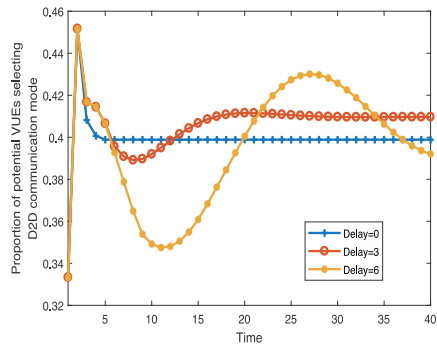


Fig. 10. Evolution of VUEs' proportion in reuse mode.

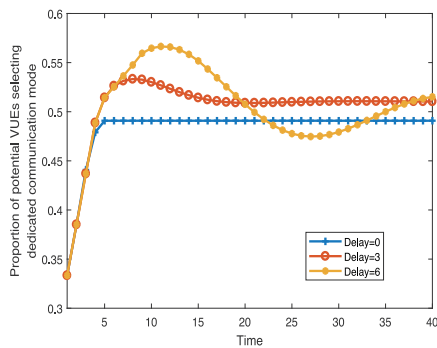


Fig. 11. Evolution of VUEs' proportion in dedicated mode.

of the equilibrium solution and the stability of the proposed framework.

4) *Optimal Dynamic Pricing*: To induce the proportion of VUEs' mode selection, the cellular BSs use the access pricing of three modes as the leader control. As the open-loop optimal dynamic pricing shown in Fig. 9, it is observed that once the proportions of VUEs in three modes evolve to be optimal, the access prices would remain the same over time.

5) *Effect of Delay on the Evolutionary Game*: Figs. 10 and 11 show the impact of delay on the iterative process of the proposed algorithm. Notice that the replicator dynamics is fluctuating when there is a delay. When there exists a small delay, e.g, 3 time slots, the population shares could still converge to the equilibrium state, while the speed is a little slow. While for the large delay, e.g, 6 time slots, the population shares keep

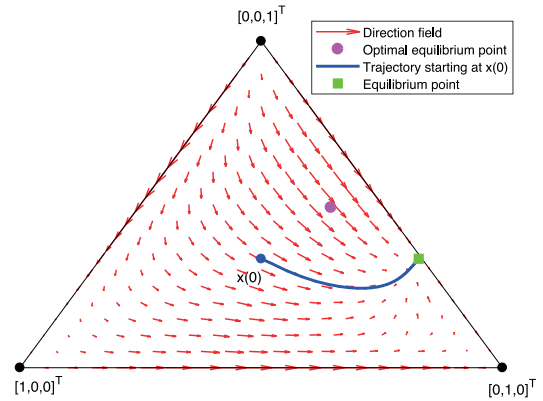


Fig. 12. Evolutionary stability without a dynamic pricing control.

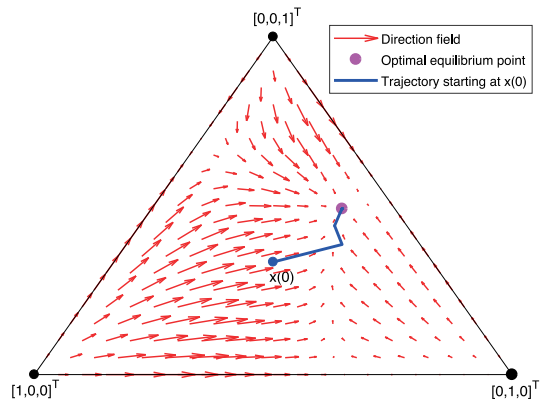


Fig. 13. Evolutionary stability with a dynamic pricing control.

fluctuating and hard to reach the equilibrium. Meanwhile, under the dynamic pricing, the population shares' evolution is driven close to the optimal distribution (as in Fig. 6), which further demonstrates the effectiveness of the proposed framework.

6) *Impact of Dynamic Pricing*: The evolutionary stability whether with or without the proposed dynamic pricing control on the proportion of potential VUEs' modes are shown in Figs. 12 and 13, respectively. In these figures, each point represents a population state, each arrow means the direction of evolution of VUEs population, and the length of each arrow implies the growth rate of population shares. Fig. 12 shows the direction field and phase trajectory of the evolutionary dynamics without the dynamic pricing control (fixed price  $[0.1, 0.7, 0.2]^T$ ) together with its EE and the optimal solution in the plane of the corresponding 2-dimensional simplex. It shows that, without a pricing mechanism, the EE point does not coincide with the optimal equilibrium state.

In Fig. 13, it can be observed that the NE obtained by the proposed dynamics pricing coincides with the optimal equilibrium point. In addition, Fig. 13 also illustrates the evolutionary stability of the proposed dynamics pricing framework. Specifically, the proportion shares of three modes with the proposed dynamics pricing are always able to converge to the optimal solution, i.e., the interior EE, from any initialization within the interior space of the simplex or can return to the optimal state

even with any small local perturbation. It is worth noting that the interior EE point is indeed the NE, which is also the evolutionary stable strategy with asymptotic stability.

### VIII. CONCLUSION

We have presented a dynamic Stackelberg pricing game framework for multi-mode selection of 5G-VANET. Specifically, we have modeled the evolution of population shares for potential VUEs by utilizing replicator dynamics of the evolutionary game. The access pricing problem of the cellular BS has been proposed as a leader control, considering the three-mode selection evolution of VUEs. The proposed framework has been shown to perform a significant performance improvement compared with various benchmark algorithms. Considering the dense deployment of small BSs in the 5G era, the joint scheduling of multiple BSs is significantly important for 5G-VANET. For future works, we will extend the performance analysis to multiple cellular BSs using software-defined networking technologies. In addition, although we have considered the highway scenario in this paper, the proposed method and the dynamic Stackelberg game framework can be extended to other scenarios. However, the mobility patterns of vehicles are unique in different scenarios, which need to be further modelled and analyzed. Therefore, the multi-mode spectrum sharing of 5G-VANET in scenarios, such as urban case and more general road system, is also our future work.

### REFERENCES

- [1] J. Gao, M. Li, L. Zhao, and X. Shen, "Contention intensity based distributed coordination for V2V safety message broadcast," *IEEE Trans. Veh. Technol.*, vol. 67, no. 12, pp. 12 288–12 301, Dec. 2018.
- [2] K. R. Malekshian and W. Zhuang, "Joint scheduling and transmission power control in wireless ad hoc networks," *IEEE Trans. Wireless Commun.*, vol. 16, no. 9, pp. 5982–5993, Sep. 2017.
- [3] H. Zhou *et al.*, "Chaincluster: Engineering a cooperative content distribution framework for highway vehicular communications," *IEEE Trans. Intell. Transp. Syst.*, vol. 15, no. 6, pp. 2644–2657, Dec. 2014.
- [4] FCC, "The FCC's 5G FAST Plan," 2019. [Online]. Available: <https://docs.fcc.gov/public/attachments/DOC-354326A1.pdf>.
- [5] H. Zhou, N. Cheng, Q. Yu, X. Shen, D. Shan, and F. Bai, "Toward multi-radio vehicular data piping for dynamic DSRC/TVWS spectrum sharing," *IEEE J. Sel. Areas Commun.*, vol. 34, no. 10, pp. 2575–2588, Oct. 2016.
- [6] B. Qian, H. Zhou, F. Lyu, J. Li, T. Ma, and F. Hou, "Toward collision-free and efficient coordination for automated vehicles at unsignalized intersection," *IEEE Internet Things J.*, vol. 6, no. 6, pp. 10 408–10 420, Dec. 2019.
- [7] F. Lyu, H. Zhu, N. Cheng, H. Zhou, W. Xu, M. Li, and X. Shen, "Characterizing urban vehicle-to-vehicle communications for reliable safety applications," *IEEE Trans. Intell. Transp. Syst.*, Jun. 2019, pp. 1–17.
- [8] Y. Li, Q. Luo, J. Liu, H. Guo, and N. Kato, "TSP security in intelligent and connected vehicles: Challenges and solutions," *IEEE Wireless Commun.*, vol. 26, no. 3, pp. 125–131, Jun. 2019.
- [9] J. Wang, J. Liu, and N. Kato, "Networking and communications in autonomous driving: A survey," *IEEE Commun. Surv. Tut.*, vol. 21, no. 2, pp. 1243–1274, Dec. 2019.
- [10] 3GPP, "3GPP Release 15," Apr. 2019, [Online] Available: <https://www.3gpp.org/release-15>
- [11] K. Abboud, H. A. Omar, and W. Zhuang, "Interworking of DSRC and cellular network technologies for V2X communications: A survey," *IEEE Trans. Veh. Technol.*, vol. 65, no. 12, pp. 9457–9470, Dec. 2016.
- [12] K. A. Hafeez, L. Zhao, B. Ma, and J. W. Mark, "Performance analysis and enhancement of the DSRC for VANET's safety applications," *IEEE Trans. Veh. Technol.*, vol. 62, no. 7, pp. 3069–3083, Sep. 2013.
- [13] H. Peng *et al.*, "Resource allocation for cellular-based inter-vehicle communications in autonomous multiplatoons," *IEEE Trans. Veh. Technol.*, vol. 66, no. 12, pp. 11 249–11 263, Dec. 2017.
- [14] H. Zhou, W. Xu, Y. Bi, J. Chen, Q. Yu, and X. Shen, "Toward 5G spectrum sharing for immersive-experience-driven vehicular communications," *IEEE Wireless Commun.*, vol. 24, no. 6, pp. 30–37, Dec. 2017.
- [15] Y. Liu, L. X. Cai, X. Shen, and H. Luo, "Deploying cognitive cellular networks under dynamic resource management," *IEEE Wireless Commun.*, vol. 20, no. 2, pp. 82–88, Apr. 2013.
- [16] J. Qiao, X. Shen, J. W. Mark, Q. Shen, Y. He, and L. Lei, "Enabling device-to-device communications in millimeter-wave 5G cellular networks," *IEEE Commun. Mag.*, vol. 53, no. 1, pp. 209–215, Jan. 2015.
- [17] X. Lin, J. G. Andrews, A. Ghosh, and R. Ratasuk, "An overview of 3GPP device-to-device proximity services," *IEEE Commun. Mag.*, vol. 52, no. 4, pp. 40–48, Apr. 2014.
- [18] H. ElSawy, E. Hossain, and M. Haenggi, "Stochastic geometry for modeling, analysis, and design of multi-tier and cognitive cellular wireless networks: A survey," *IEEE Commun. Surv. Tut.*, vol. 15, no. 3, pp. 996–1019, Jul. 2013.
- [19] S. Li and J. Huang, "Price differentiation for communication networks," *IEEE/ACM Trans. Netw.*, vol. 22, no. 3, pp. 703–716, Jun. 2014.
- [20] H. ElSawy, E. Hossain, and M. Alouini, "Analytical modeling of mode selection and power control for underlay D2D communication in cellular networks," *IEEE Trans. Commun.*, vol. 62, no. 11, pp. 4147–4161, Nov. 2014.
- [21] N. Cheng *et al.*, "Performance analysis of vehicular device-to-device underlay communication," *IEEE Trans. Veh. Technol.*, vol. 66, no. 6, pp. 5409–5421, Jun. 2017.
- [22] K. Zheng, Q. Zheng, P. Chatzimisios, W. Xiang, and Y. Zhou, "Heterogeneous vehicular networking: A survey on architecture, challenges, and solutions," *IEEE Commun. Surv. Tut.*, vol. 17, no. 4, pp. 2377–2396, Jun. 2015.
- [23] K. Zhu and E. Hossain, "Joint mode selection and spectrum partitioning for device-to-device communication: A dynamic Stackelberg game," *IEEE Trans. Wireless Commun.*, vol. 14, no. 3, pp. 1406–1420, Mar. 2015.
- [24] R. Ma, N. Xia, H. Chen, C. Chiu, and C. Yang, "Mode selection, radio resource allocation, and power coordination in D2D communications," *IEEE Wireless Commun.*, vol. 24, no. 3, pp. 112–121, Jun. 2017.
- [25] Y. Wu, T. Zhang, and D. H. K. Tsang, "Joint pricing and power allocation for dynamic spectrum access networks with Stackelberg game model," *IEEE Trans. Wireless Commun.*, vol. 10, no. 1, pp. 12–19, Jan. 2011.
- [26] A. Omri and M. O. Hasna, "A distance-based mode selection scheme for D2D-enabled networks with mobility," *IEEE Trans. Wireless Commun.*, vol. 17, no. 7, pp. 4326–4340, Jul. 2018.
- [27] D. Niyato and E. Hossain, "Dynamics of network selection in heterogeneous wireless networks: An evolutionary game approach," *IEEE Trans. Veh. Technol.*, vol. 58, no. 4, pp. 2008–2017, May 2009.
- [28] Q. Zheng, K. Zheng, H. Zhang, and V. C. M. Leung, "Delay-optimal virtualized radio resource scheduling in software-defined vehicular networks via stochastic learning," *IEEE Trans. Veh. Technol.*, vol. 65, no. 10, pp. 7857–7867, Oct. 2016.
- [29] C. Xu *et al.*, "Efficiency resource allocation for device-to-device underlay communication systems: A reverse iterative combinatorial auction based approach," *IEEE J. Sel. Areas Commun.*, vol. 31, no. 9, pp. 348–358, Sep. 2013.
- [30] M. K. Hanawal, E. Altman, and F. Baccelli, "Stochastic geometry based medium access games in wireless ad hoc networks," *IEEE J. Sel. Areas Commun.*, vol. 30, no. 11, pp. 2146–2157, Dec. 2012.
- [31] G. Bianchi, "Performance analysis of the IEEE 802.11 distributed coordination function," *IEEE J. Sel. Areas Commun.*, vol. 18, no. 3, pp. 535–547, Mar. 2000.
- [32] D. Tian, J. Zhou, Y. Wang, Z. Sheng, X. Duan, and V. C. M. Leung, "Channel access optimization with adaptive congestion pricing for cognitive vehicular networks: An evolutionary game approach," *IEEE Trans. Mobile Comput.*, vol. 19, no. 4, pp. 803–820, Apr. 2020.
- [33] K. Ciesielski, "On Stefan Banach and some of his results," *Banach J. Math. Anal.*, vol. 1, pp. 1–10, Sep. 2007.
- [34] J. Gondzio and T. Terlaky, "A computational view of interior-point methods for linear programming," *Adv. Linear Integer Program.*, vol. 36, no. 3, pp. 103–144, Nov. 1994.
- [35] R. G. Bartle, "Return to the Riemann integral," *Amer. Math. Monthly*, vol. 103, no. 8, pp. 625–632, Oct. 1996.
- [36] P. A. Lopez *et al.*, "Microscopic traffic simulation using SUMO," in *Proc. 21st Int. Conf. Intell. Transp. Syst.*, Nov. 2018, pp. 2575–2582.



**Bo Qian** (Student Member, IEEE) received the B.S. and M.S. degrees in statistics from Sichuan University, Chengdu, China, in 2015 and 2018, respectively. He is currently working toward the Ph.D. degree with the School of Electronic Science and Engineering, Nanjing University, China. His current research interests include intelligent transportation systems and vehicular networks, wireless resource management, blockchain, convex optimization theory and game theory.



**Kai Yu** (Student Member, IEEE) received the B.S. degree in detection, guidance and control technology from the University of Electronic Science and Technology of China, Chengdu, China, in 2019. He is currently working toward the Ph.D. degree in communications and information system with Nanjing University, Nanjing, China. His research interests include resource allocation, machine learning for wireless communications, and heterogeneous cellular networks.



**Haibo Zhou** (Senior Member, IEEE) received the Ph.D. degree in information and communication engineering from Shanghai Jiao Tong University, Shanghai, China, in 2014. From 2014 to 2017, he was a Postdoctoral Fellow with the Broadband Communications Research Group, Department of Electrical and Computer Engineering, University of Waterloo. He is currently an Associate Professor with the School of Electronic Science and Engineering, Nanjing University, Nanjing, China. His research interests include resource management and protocol design in vehicular



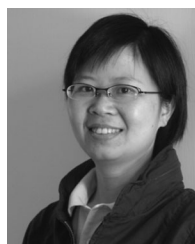
**Xuemin (Sherman) Shen** (Fellow, IEEE) received the Ph.D. degree in electrical engineering from Rutgers University, New Brunswick, NJ, USA, in 1990. He is currently a University Professor with the Department of Electrical and Computer Engineering, University of Waterloo, Canada. His research focuses on network resource management, wireless network security, Internet of Things, 5G and beyond, and vehicular ad hoc and sensor networks. He is a registered Professional Engineer of Ontario, Canada, an Engineering Institute of Canada Fellow, a Canadian

ad hoc networks, cognitive networks and space-air-ground integrated networks. He was a recipient of the 2019 IEEE ComSoc Asia-Pacific Outstanding Young Researcher Award. He served as an Invited Track Co-Chair for ICC'2019, VTC-Fall'2020 and a TPC Member of many IEEE conferences, including GLOBECOM, ICC, and VTC. He served as an Associate Editor for the IEEE Comsoc Technically Co-Sponsored the Journal of Communications and Information Networks (JCIN) from April 2017 to March 2019, and a Guest Editor for the *IEEE Communications Magazine* in 2016, the *Hindawi International Journal of Distributed Sensor Networks* in 2017, and *IET Communications* in 2017. He is currently an Associate Editor of the *IEEE Internet of Things Journal*, the *IEEE Network Magazine*, and the IEEE WIRELESS COMMUNICATIONS LETTER.

Academy of Engineering Fellow, a Royal Society of Canada Fellow, and a Distinguished Lecturer of the IEEE Vehicular Technology Society and Communications Society. Dr. Shen received the R.A. Fessenden Award in 2019 from IEEE, Canada, James Evans Avant Garde Award in 2018 from the IEEE Vehicular Technology Society, Joseph LoCicero Award in 2015 and Education Award in 2017 from the IEEE Communications Society. He has also received the Excellent Graduate Supervision Award in 2006 and Outstanding Performance Award five times from the University of Waterloo and the Premier's Research Excellence Award (PREA) in 2003 from the Province of Ontario, Canada. He served as the Technical Program Committee Chair/CoChair for the IEEE Globecom'16, the IEEE Infocom'14, the IEEE VTC'10 Fall, the IEEE Globecom'07, the Symposia Chair for the IEEE ICC'10, and the Chair for the IEEE Communications Society Technical Committee on Wireless Communications. He was the Editor-in-Chief of the IEEE INTERNET OF THINGS JOURNAL and IEEE Network, and the Vice President on Publications of the IEEE Communications Society.



**Ting Ma** (Student Member, IEEE) received the B.S. and M.S. degrees in statistics in 2013 and 2016, respectively, from Sichuan University, Chengdu, China, where she is currently working toward the Ph.D. degree. Her current research interests mainly include robust hypothesis testing, algorithm design and analysis with applications in signal processing, convex optimization theory and game theory.



**Fen Hou** (Member, IEEE) received the Ph.D. degree in electrical and computer engineering from the University of Waterloo, Waterloo, Canada, in 2008. She was a Postdoctoral Fellow in electrical and computer engineering with the University of Waterloo, from 2008 to 2009, and also with the Department of Information Engineering, Chinese University of Hong Kong, from 2009 to 2011. She is currently an Associate Professor with the Department of Electrical and Computer Engineering, University of Macau.

Her research interests include resource allocation and scheduling in broadband wireless networks, protocol design and QoS provisioning for multimedia communications in broadband wireless networks, mechanism design and optimal user behavior in mobile crowd sensing networks, and mobile data offloading. She was a recipient of the IEEE Globecom Best Paper Award in 2010 and the Distinguished Service Award in the IEEE MMTC in 2011. She served as the Co-Chair of the ICCS 2014 Special Session on Economic Theory and Communication Networks, the INFOCOM 2014 Workshop on Green Cognitive Communications and Computing Networks, the IEEE Globecom Workshop on Cloud Computing System, Networks, and Application 2013 and 2014, the ICC 2015 Selected Topics in Communications Symposium, and the ICC 2016 Communication Software Services and Multimedia Application Symposium. She currently serves as the Director of Award Board in IEEE ComSoc Multimedia Communications Technical Committee. She also serves as an Associate Editor of *IET Communications*.



**Yunting Xu** (Student Member, IEEE) received the B.S. degree in communication engineering from Nanjing University, Nanjing, China in 2017. He is currently working toward the M.S. degree with the School of Electronic Science and Engineering, Nanjing University. His research interests include the study of intersection scheduling in the field of vehicular ad hoc networks and intelligent transportation systems.